Hydrothermal sensitivities of seed populations underlie fluctuations of dormancy states in an annual plant community

Shuangshuang Liu (iD),[1,2] Kent J. Bradford,[2] Zhenying Huang (iD),[3,5] and D. Lawrence Venable[4]

[1]*Ministry of Education Key Laboratory for Biodiversity Science and Ecologic Engineering, Institute of Biodiversity Science, Fudan University, Shanghai 200438 China*
[2]*Department of Plant Sciences, Seed Biotechnology Center, University of California, Davis, California 95616 USA*
[3]*State Key Laboratory of Vegetation and Environmental Change, Institute of Botany, Chinese Academy of Sciences, Beijing 100093 China*
[4]*Department of Ecology and Evolutionary Biology, University of Arizona, Tucson, Arizona 85721 USA*

Abstract. Plant germination ecology involves continuous interactions between changing environmental conditions and the sensitivity of seed populations to respond to those conditions at a given time. Ecologically meaningful parameters characterizing germination capacity (or dormancy) are needed to advance our understanding of the evolution of germination strategies within plant communities. The germination traits commonly examined (e.g., maximum germination percentage under optimal conditions) may not adequately reflect the critical ecological differences in germination behavior across species, communities, and seasons. In particular, most seeds exhibit primary dormancy at dispersal that is alleviated by exposure to dry after-ripening or to hydrated chilling to enable germination in a subsequent favorable season. Population-based threshold (PBT) models of seed germination enable quantification of patterns of germination timing using parameters based on mechanistic assumptions about the underlying germination physiology. We applied the hydrothermal time (HTT) model, a type of PBT model that integrates environmental temperature and water availability, to study germination physiology in a guild of coexisting desert annual species whose seeds were after-ripened by dry storage under different conditions. We show that HTT assumptions are valid for describing germination physiology in these species, including loss of dormancy during after-ripening. Key HTT parameters, the hydrothermal time constant (θ_{HT}) and base water potential distribution among seeds ($\Psi_b(g)$), were effective in describing changes in dormancy states and in clustering species exhibiting similar germination syndromes. θ_{HT} is an inherent species-specific trait relating to timing of germination that correlates well with long-term field germination fraction, while $\Psi_b(g)$ shifts with depth of dormancy in response to after-ripening and seasonal environmental variation. Predictions based on variation among coexisting species in θ_{HT} and $\Psi_b(g)$ in laboratory germination tests matched well with 25-yr observations of germination dates and fractions for the same species in natural field conditions. Seed dormancy and germination strategies, which are significant contributors to long-term species demographics under natural conditions, can be represented by readily measurable functional traits underlying variation in germination phenologies.

Key words: after-ripening; dormancy; germination niche; germination phenology; hydrothermal time model; plant functional trait.

Introduction

The diversity of seed germination phenologies among species is a widely documented natural phenomenon (Baskin and Baskin 2014). Important both ecologically and evolutionarily, germination timing sets the context for subsequent development and fitness in plants. For example, germination timing is associated with postgermination traits such as the rosette size at reproduction in *Arabidopsis thaliana* (Donohue 2002) and the timing of flowering (e.g., annual or biennial life cycles) in *Campanulastrum americanum* (Galloway 2001, 2002), influencing strength and mode of selection. Previous studies have shown that germination time has variable effects on fitness at different life stages (Donohue et al. 2010) and in different years (Gremer et al. 2016) depending on the timing of resource pulses and lethal environmental conditions. Moreover, seed dormancy has been shown to

affect plant life history independently of its effects on germination time (de Casas et al. 2012, Huo et al. 2016).

Germination timing is also a critical contributor to plant population dynamics and species coexistence through its interactions with other plant developmental stages, functional traits, and the environment (Clauss and Venable 2000, Donohue et al. 2005, Angert et al. 2009). For example, in a Sonoran Desert winter annual plant community, species with high water-use efficiency and less interannual demographic variability germinated and reproduced earlier in the season (Kimball et al. 2011). The growth-phase physiology and phenology characteristics among species are correlated with differential germination, survival, and reproduction in response to variation in weather conditions across years. This species-by-year interaction promotes species coexistence via the storage effect (Angert et al. 2009, Huang et al. 2016). In this annual plant community, variation in germination timing within and among years also reflects adaptive predictive germination plasticity and bet-hedging strategies (Gremer et al. 2016). Predictive germination leads to germination in favorable conditions and improves individual fitness, whereas bet hedging spreads the risk of germination and sacrifices mean fitness to reduce variance in fitness (Cohen 1966, Simons 2011).

An important process that affects the variation in germination timing is after-ripening, the decrease in seed physiological dormancy with time during dry storage (Holdsworth et al. 2008). The molecular mechanisms by which germination potential increases during dry aging remain essentially unknown (Long et al. 2015), but may be associated with oxidation of germination inhibitors (Bazin et al. 2011). The loss of dormancy due to after-ripening is accompanied by marked changes in the sensitivity "windows" of germination to external and internal signals following imbibition (Alvarado and Bradford 2005, Finch-Savage and Leubner-Metzger 2006). After-ripening is especially important in the adaptation of annual plants to cyclic drought conditions by preventing premature germination during intermittent rainfall in a dry season, yet preparing fractions of the seed population for rapid germination once adequate rainfall occurs in a wet season (Baskin and Baskin 2014). In addition, after-ripening may serve as the functional link connecting germination strategies with the evolution of plant life history traits in variable environments. For example, *Arabidopsis* seeds that germinated following different lengths of after-ripening exhibited physiological and phenotypic heterogeneity (and thus variation in fitness) among the seedlings (de Casas et al. 2012).

Characterizing the functional properties of germination is complex because various aspects are involved, such as the optimal environmental conditions required; the fraction of germinable individuals at a given time; and the speed, uniformity, and percentage of germination under the prevailing conditions. This poses challenges for quantitatively characterizing and comparing germination among species. Thus, a set of physiologically based and ecologically meaningful parameters describing aspects of germination physiology are desired. When a given seed will be triggered to germinate depends upon its individual physiological condition (e.g., genetic and maternal effects) and its sensitivity to current environmental conditions, which are essentially impossible to predict for an individual seed. Thus, physiological or functional characterization of seed biology must be based on the distribution of physiological states or germination behaviors among seeds in a population (Roberts 1973, Bradford 2018). The characteristic right-skewed sigmoid pattern of cumulative germination percentages of a seed population under a wide range of conditions can be well described by population-based models utilizing a normal frequency distribution of parameters (Bello and Bradford 2016, Bradford 2018). Such models can characterize not only the average behavior, but also the variability among individuals in their germination timing, which is a critical component of an opportunistic versus a bet-hedging strategy and sets the stage for the subsequent phenotypic and fitness variation in the germinants. These models are collectively referred to as "population-based threshold" (PBT) models, notably the thermal time (TT), hydrotime (HT), and hydrothermal time (HTT) models (Garcia-Huidobro et al. 1982, Gummerson 1986, Bradford 1990, Alvarado and Bradford 2002, Batlla and Benech-Arnold 2015, Donohue et al. 2015, Bello and Bradford 2016).

Central to PBT models are the hypotheses that (1) seed populations exhibit intrinsic, generally (but not necessarily) normal distributions of sensitivity thresholds such as for temperature (T) and water potential (Ψ) that govern their germination responses to these environmental factors; (2) the effects of environmental factors are cumulative over time in proportion to the extent by which the factor (T or Ψ) exceeds each seed's sensitivity threshold value; and (3) a seed germinates when the environmental dose it has accumulated surpasses its total TT, HT, or HTT requirements (Gummerson 1986). By recording germination time courses across a gradient of environmental conditions, the distribution of sensitivity thresholds and the total factor-time requirements can be determined and then used to predict germination fraction and timing in a range of specified environments (Bradford 1995, 2018, Donohue et al. 2015). Sensitivity thresholds can also be measured for a variety of factors in addition to T and Ψ, such as germination responses to oxygen and light (reviewed in Bradford 2018).

The general application of PBT analyses to diverse species is supported by extensive studies (reviewed in Allen et al. 2007, Bewley et al. 2013, Dürr et al. 2015). However, few studies have followed the lead of Allen et al. (2000) (Meyer and Allen 2009) and explored the application of PBT models to identify the potential links between germination physiology and field germination strategies in coexisting species that compete for limited resources in a variable environment. A recent study applied TT and HT models

to germination behavior in the same guild of desert annual plants as mentioned above (Huang et al. 2016). In this system, germination behavior is an important adaptive strategy to cope with environmental variation (Cohen 1966, Venable 2007, Gremer and Venable 2014, Gremer et al. 2016). PBT models enabled detailed description of germination responses to T and Ψ, which were linked to a number of functional and population dynamic traits that characterize the complex life history strategies in this community. For example, species with slow-germination functional traits (i.e., high median thermal time constant [$\theta_T(50)$] and median base water potential [$\Psi_b(50)$]) tended to have small seeds and low seedling to adult survival but high seed production in plants that survived to maturity. They also have low field germination fractions and integrated water-useefficiencies but high relative growth rates and demographic variation (Huang et al. 2016). Species with fast-germination functional traits showed the opposite associations. Over a 22-yr period, variation in germination fraction was a significant determinant of year-to-year changes in population size for 8 of 13 speciesand was a stronger determinant than variation in survival or fecundity for 5 of 13 species (Huang et al. 2016). Overall, these results demonstrate the prominent role germination plays (along with survival and fecundity) in population size changes in this community.

However, Huang et al. (2016) did not explore the dormancy alleviation/cycling process (i.e., the change of dormancy state) during after-ripening, which is an important life history trait in this desert annual community (Adondakis and Venable 2004). Dormancy cycling has been suggested as an important adaptation to specific habitats (Baskin and Baskin 1985, Baskin et al. 1993, Finch-Savage and Footitt 2017), and is found in diverse plant forms in addition to annual plants (e.g., Cao et al. 2014, Copete et al. 2015). Huang et al. (2016) reported only on seeds that had been after-ripened for 4–5.5 months and therefore had largely lost the primary dormancy present in freshly matured seeds. Maintenance of primary dormancy through the summer may prevent lethal germination due to erratic monsoon rainfall, and the extent of alleviation of dormancy before and during the main germination season (October–January; Gremer et al. 2016) would determine the fraction of the seed bank physiologically capable of germinating at different times. Seeds that do not germinate during the favorable time window can be induced into secondary dormancy to delay or prevent germination until a subsequent environmental opportunity (Adondakis and Venable 2004). Patterns of changes of dormancy states during after-ripening can be characterized by PBT models, which have been used in describing dormancy loss in *Bromus tectorum* in relation to field germination ecology (Christensen et al. 1996, Bauer

et al. 1998), after-ripening in botanical potato seeds (Alvarado and Bradford 2005), and secondary dormancy induction in *Polygonum aviculare* seeds (Batlla and Agostinelli 2017).

It is more difficult to apply TT and HT models to study changes of dormancy states during after-ripening because many species are very dormant in early after-ripening months and germinate poorly in lower water-potential treatments, limiting the data available to fit HT models. Fortunately, the combined effects of T and Ψ may be examined via HTT models, which assume that individuals in a seed population share a common hydrothermal time constant (θ_{HT}) that does not change with environmental conditions (Gummerson 1986, Alvarado and Bradford 2002, 2005). The HTT model has adequately described germination behavior of diverse species (Dahal and Bradford 1994, Kebreab and Murdoch 1999, Grundy et al. 2000, Bradford 2002, Finch-Savage et al. 2005, Bloomberg et al. 2009, Onofri et al. 2018). Notably, Köchy and Tielbörger (2007) used a simplified HTT approach to estimate parameter values for 74 annual plant species originating from four climates in Israel. Assuming that θ_{HT} is an inherent seed population trait and stays constant across dormancy states, once its value is determined from after-ripened seeds, we can apply the HTT model to estimate changes in parameters for the Ψ threshold distribution during after-ripening (see Methods).

To understand the relationship between field germination ecology and germination physiology in response to after-ripening, we used HTT models to characterize quantitatively the combined effects of T and Ψ on dormancy states and fluctuations during after-ripening in the same guild of desert annuals studied by Huang et al. (2016). First we asked (Question 1), are there species-specific patterns of dormancy fluctuations (revealed by germination behavior in T and Ψ treatments) in response to after-ripening in a community of desert winter annuals? Secondly (Question 2), do assumptions of the HTT model hold in the desert annual plant system and can we use model parameters to describe germination syndromes and compare patterns of dormancy fluctuations among species? Lastly (Questions 3), do species' germination and dormancy traits during after-ripening correlate with field germination strategies? Specifically, do high θ_{HT} and Ψ_b (base water potential) values and small changes in Ψ_b distribution during after-ripening, which indicate slow germination, high dormancy state, and slow dormancy alleviation, associate with small field germination fraction and/or late germination date? Overall, we aim to apply a quantitative physiological and functional perspective to identify variation among coexisting species in germination and dormancy strategies in response to after-ripening, and determine how such strategies may relate to field germination traits. This link between dormancy fluctuations during after-ripening and field germination ecology constitute a critical element of the life history strategies of desert annual plants to cope with highly variable environments.

Materials and Methods

Study system

Field work was conducted in the Sonoran Desert at the University of Arizona's Desert Laboratory at Tumamoc Hill, Tucson, Arizona, USA (32°13′ N, 111°0′ W). The 13 species selected, including 1 with three morphological seed types, represent common winter annuals at this site: *Draba cuneifolia* (DRCU), *Erodium cicutarium* (ERCI), *Eriophyllum lanosum* (ERLA), *Erodium texanum* (ERTE), *Eucrypta micrantha* (EUMI), *Evax multicaulis* (EVMU), *Pectocarya heterocarpa* Basal (PEHE-B), Long (PEHE-L), and Winged (PEHE-W) seed types, *Pectocarya recurvata* (PERE), *Plantago ovata* var. *insularis* (PLIN), *Plantago patagonica* (PLPA), *Schismus barbatus* (SCBA), *Stylocline micropoides* (STMI), and *Festuca* (formerly *Vulpia*) *octiflora* (VUOC). These species constitute 68% of all winter annuals seen at the Desert Laboratory collection site during the past 30 yr. This desert ecosystem has strong interannual variation in rainfall. In addition, 50% of the species in local Sonoran Desert floras are annuals that play an important role in responding to the environmental fluctuation and passing it on to higher trophic levels (reviewed in Venable and Pake 1999). Germination of these winter annuals usually occurs sometime between October and January, and seeds mature between late February and early April at this site. Seeds typically have primary dormancy and require dry after-ripening at high temperature for dormancy loss (Adondakis and Venable 2004).

After-ripening treatments and germination tests

Freshly matured seeds were collected from 50–100 plants between April 10 and May 10, 2010. Seeds were stored under three after-ripening conditions to alleviate primary dormancy: (1) natural field conditions (protected from rain; see Huang et al. 2016 for field storage details), (2) constant 30°C, and (3) 45°C temperatures in ovens. Germination tests were conducted on seeds stored for 0 (fresh seeds), 1, 2, 3, and 4 months. Several species had low germination percentages after 4 months of after-ripening, and were after-ripened an additional 1.5 months (i.e., 5.5 months total). *Erodium cicutarium* (ERCI) and *Erodium texanum* (ERTE) have combined physical and physiological dormancy, so seed coats were removed to investigate only physiological dormancy.

For seeds after-ripened in the field and at 45°C for 4 or 5.5 months, germination was tested at a combination of *T* (between 8°C and 35°C) and Ψ (between 0 and −1.0 MPa) conditions appropriate for each species (seeds after-ripened at 30°C were germinated only at 0 MPa). Water potential was controlled using PEG 8000 solutions (Ampresco, Solon, Ohio, USA) prepared according to Michel (1983). For seeds after-ripened for 0, 1, 2, and 3 months, germination was tested under the same gradient of temperatures but only in water

(0 MPa). During those storage times, many species exhibited dormancy and germination was low at more negative water potentials (see Supplemental Data). There were four replications of 25 seeds for each treatment combination per species. Seeds were incubated in plastic petri dishes (5-cm diameter) under constant *T* in light for 20 d. Germination was examined every 12, 24, or 48 h according to the germination speed of each species (every 4 h initially for fast germinators), and germination was recorded at radicle emergence. At the end of the germination experiment, the viability of nongerminated seeds was tested by 1% triphenyl tetrazolium chloride (Baskin and Baskin 2014). Results showed that in all species tested, no nongerminated seeds had lost viability. Further details of the after-ripening treatments and germination tests are described in the supplemental materials of Huang et al. (2016).

Hydrothermal time (HTT) model and extensions

HTT models assume a single common hydrothermal time constant (θ_{HT}) for all individual seeds within a population as defined in Eq. 1 (Gummerson 1986):

$$\theta_{HT} = (\psi - \psi_{b(g)})(T - T_b)t_g. \tag{1}$$

Ψ and *T* represent the external water potential and temperature, respectively, at which seeds are incubated. $\Psi_b(g)$ is the base (i.e., threshold or most negative) water potential just permitting germination of a specific fraction g (e.g., 16%, 50%, etc.) of the seed population, and the $\Psi_b(g)$ values for a seed population are assumed to exhibit a normal distribution. For example, $\Psi_b(50)$ is the base water potential threshold for the 50th percentile of the seed population, meaning that when external Ψ equals $\Psi_b(50)$, a maximum of only 50% of seeds can germinate. T_b is the base temperature for germination and is assumed here to be constant for all seeds within the population. Within a sub-optimal temperature range for germination (i.e., between base temperature T_b and the optimal temperature T_0), we assume that $\Psi_b(g)$ does not change significantly with temperature (Alvarado and Bradford 2002).

When *T* exceeds T_0, the HTT model assumes that $\Psi_b(g)$ increases with temperature, which results in smaller values of $\Psi - \Psi_b(g)$ and therefore longer times to germination until it is prevented at the ceiling temperature (T_c), which varies among seeds in the population (Alvarado and Bradford 2002). The increase in $\Psi_b(g)$ with increasing supra-optimal temperature is given by $k_T (T - T_0)$, where k_T is a constant (Eq. 2) (Alvarado and Bradford 2002).

$$\theta_{HT} = \left\{ \psi - \psi_{b(g)} - [k_T(T - T_0)] \right\}(T_0 - T_b)t_g. \tag{2}$$

The $k_T(T - T_0)$ term is included only for supra-optimal temperatures. At those temperatures, the population may not accumulate additional temperature dose

beyond that at T_0, so $(T_0 - T_b)t_g$ is used instead of $(T - T_b)t_g$ in Eq. 2 when $T > T_0$ (but see also Rowse and Finch-Savage 2003, Watt et al. 2011, Watt and Bloomberg 2012, Mesgaran et al. 2017).

In this work we focused primarily on HTT at suboptimal T, because supra-optimal HTT is essentially an adjustment of $\Psi_b(g)$ as estimated from the sub-optimal HTT. In addition, the germination season in this system usually falls between October and January (Venable 1999), during which the average temperature ranges from 11.1°C to 15.7°C, below T_0 for most of the species (Huang et al. 2016). Supra-optimal HTT parameters were estimated only for seeds after-ripened for 4–5.5 m and were used in the clustering analysis and simulation of germination niches.

Following HTT assumptions, cumulative germination fractions (g) correspond to the integral of the normal distribution of $\Psi_b(g)$, which can be characterized by two parameters, its median ($\Psi_b(50)$) and standard deviation ($\sigma_{\Psi b}$). A probit transformation (Bliss 1934) linearizes a cumulative normal distribution with slope of $\sigma_{\Psi b}$ (Eq. 3), so incorporating (1) and (3) leads to Eq. 4:

$$\text{Probit}(g) = (\psi_b(g) - \psi_b(50))/\sigma\psi_b \quad (3)$$

$$\text{Probit}(g) = \{\psi - [\theta_{HT}/(T - T_b)t_g] - \psi_b(50)\}/\sigma\psi_b. \quad (4)$$

With values of g, t_g, Ψ, and T obtained from germination tests under a combination of water potentials and temperatures and using the relationship between θ_{HT}, T_b, and $\Psi_b(g)$ given in Eq. 1, we can find the values of θ_{HT} and T_b that give the best fit to a linear regression of probit (g) on $\Psi_b(g)$ (i.e., maximizes the R^2; Bradford 1990). Specifically, we first set starting values of θ_{HT} and T_b for a species based on inspection of its germination data. Then for each germination percentage g recorded at a specific time for a water potential-by-temperature treatment, a predicted value of $\Psi_b(g)$ was calculated via $\Psi_b(g) = \Psi - [\theta_{HT}/(T - T_b) t_g]$ and regressed versus the probit value of g (converted from decimal fraction using the "NORMSINV" function in Excel [Version 14.5.5]). Because HTT assumes a linear relationship between $\Psi_b(g)$ and probit(g), the best values of θ_{HT} and T_b were found when the R^2 between $\Psi_b(g)$ and probit(g) was maximized. The process of optimizing R^2 by varying both θ_{HT} and T_b was nonlinear and was conducted in Excel (Version 14.5.5) with the "Solver" plug-in, based on a generalized reduced gradient (GRG) nonlinear optimization (Lasdon et al. 1978). Once the best estimates of θ_{HT} and T_b were determined, which resulted in the best-fitting regression of probit(g) on $\Psi_b(g)$, the values of $\Psi_b(50)$ and $\sigma_{\Psi b}$ were calculated from the slope and intercept of the linear regression using Eq. 3. A significant linear relationship between probit (g) and $\Psi_b(g)$ indicates that the HTT assumptions (Eqs. 1 and 3) are valid for the data set tested.

We estimated parameters θ_{HT}, $\Psi_b(50)$, $\sigma_{\Psi b}$, T_b, T_0, and k_T via HTT models (Eqs. 1 and 2) for seeds after-ripened for 4 or 5.5 months in the field and at 45°C, where $\Psi_b(50)$ is the median Ψ_b threshold and $\sigma_{\Psi b}$ is the standard deviation of Ψ_b. We assume that θ_{HT} does not change in a seed population when dormancy states fluctuate (Allen and Meyer 2002). In a separate analysis, these parameters were used as starting values to fit HTT after-ripening models for seeds tested at 1-month increments from 0 to 5.5 months in all three after-ripening conditions (germination tested only in water, $\Psi = 0$ MPa). θ_{HT} and T_b were kept constant, while $\Psi_b(50)$ and $\sigma_{\Psi b}$ were allowed to vary, until a best fit was found and the average sums of squares of residuals between observed germination fraction and predicted germination fraction were minimized (the fitting process also used the "Solver" plug-in in Excel). Seeds after-ripened at 30°C were only germinated at 0 MPa; thus estimates of θ_{HT} from seeds after-ripened in the field were used for modeling $\Psi_b(50)$ and $\sigma_{\Psi b}$ of 30°C–after-ripened seeds. For several very dormant species, germination data were insufficient for model fitting until the third or fourth month.

K-means clustering analysis and principal-component analysis (PCA) were performed in R (version 3.5.1) with HTT parameters (θ_{HT}, T_b, T_0, k_T, $\Psi_b(50)$, and $\Psi_b(50)$ and $\sigma_{\Psi b}$ for seeds after-ripened from 0 to 4 months), to separate the 15 species into distinctive germination groups.

Germination rate and after-ripening rate

Germination rate (GR(g)) is defined as $1/t_g$ and can be obtained from HTT parameters by rearranging Eqs. 1 and 3 to give Eqs. 5 and 6:

$$\text{GR}(g) = [(\psi - \psi_{b(g)})(T - T_b)]/\theta_{HT}) \quad (5)$$

$$\text{GR}(g) = [(\psi - (\text{probit}(g) \cdot \boldsymbol{\sigma}\psi_b) - \psi_b(50))(T - T_b)]/\theta_{HT}. \quad (6)$$

For comparison among species, some of which did not germinate to 50%, we estimated the time to 16% germination using Eq. 7:

$$\text{GR}(16) = [(\psi - (\text{probit}(16) \cdot \boldsymbol{\sigma}\psi_b) - \psi_{\boldsymbol{b}}(50))(T - T_b)]/\theta_{HT} \quad (7)$$

to calculate GR(16) (= $1/t_{16}$). This fraction contains seeds for which the $\Psi_b(g)$ thresholds are one standard deviation more negative than the median values (g = 50%), and therefore represents the seeds that germinate more rapidly after imbibition.

After-ripening rate (AR(g)) is calculated as the change of dormancy state per unit time, defined as change of GR(g) from an earlier stage $(\text{GR}(g)_E)$ to a later stage $(\text{GR}(g)_L)$. As GR increases with AR time, to result in positive values we defined AR(16) as

$$AR(16) = GR(16)_L - GR(16)_E \qquad (8)$$

where the GR(16) values at each AR time are calculated as above. We calculated AR(16) for every two consecutive months of after-ripening times for each species. In addition, we compared maximum AR(16) (the maximum value of AR(16) across months for a species) to average field germination fraction. Although maximum AR may not accurately describe the exact kinetics of dormancy loss during the course of the experiment, it captures the species' maximum capacity for responsiveness to after-ripening (dormancy loss) during its most sensitive time period.

Simulation of germination niches

With HTT parameters (θ_{HT}, $\Psi_b(50)$, $\sigma_{\Psi b}$, T_b, T_0 and k_T) estimated from 4 to 5.5-months field–after-ripened seeds, we calculated probit(g) for each species for an environmental range of combined water potentials (Ψ = 0 to −1.2 MPa) and temperatures (T = 6–24°C) within 5 d of imbibition (t = 0–120 h) (Eq. 4). The conversion of probit(g) to germination percentage gives g at a specific time t_g and environmental condition. Water potentials, temperatures, and times were set to simulate realistic environmental conditions for germination events following a precipitation event during the germination season at the Desert Laboratory field site.

Field germination data

Field germination fraction was calculated by estimating seedling density (m^{-2}) of each species from long-term field plots, combining it with ungerminated seed density (m^{-2}) from soil seedbank sampling at the end of the germination season, and averaging over 25 yr (1990–2014; details in Gremer et al. 2016). Mean germination date was calculated as the average germination census date of seeds that germinated (germination censuses were conducted 7–10 d after the start of each rainfall event, by which time most seedlings in a cohort will have emerged). These mean germination dates were then averaged over the same 25-yr period (Huang et al. 2016). The potential correlations between field germination traits (germination fraction and mean germination date) and HTT parameters were analyzed via Pearson correlation tests in R (version 3.5.1).

Results

HTT model fitting

The HTT model explained germination data well for the 4 or 5.5 months, field and 45°C–after-ripened seeds (R^2 values from 0.80 to 0.95 for sub-optimal and 0.61–0.97 for supra-optimal temperature range; Table 1). However, there were a few cases where the model underestimated (e.g., EVMU at −0.3 MPa, STMI at −0.3 MPa) or overestimated (e.g., ERTE at −0.3 MPa) germination percentages at lower water potentials (Appendix S1: Fig. S1). After-ripening models (holding θ_{HT} constant and using temperature treatments to estimate changes in $\Psi_b(50)$ and $\sigma_{\Psi b}$) also matched germination data well in most species (R^2 values between 0.71 and 0.99; Table 1).

Species displayed diverse values for θ_{HT} and $\Psi_b(g)$ distributions. For field–after-ripened seeds, θ_{HT} varied between 260 and 2,150 (MPa·°C·h), $\Psi_b(50)$ between −2.62 and 0.19 MPa and $\sigma_{\Psi b}$ between 0.16 and 0.69 MPa. Base temperatures for germination (T_b) were near 0°C for all species. The k_T values, indicating the sharpness with which germination was reduced as T increased above T_0, varied among the individual species (Table 1). Final estimates of θ_{HT} for seeds after-ripened at 45°C for 4–5.5 months were similar to those for seeds after-ripened in the field, except for four species (VUOC, SCBA, DRCU, and ERCI) that had higher values with 45°C after-ripening. In general, for species in which Ψ_b distributions changed because of after-ripening, their median values shifted to more negative values with increasing after-ripening durations (Table 1, Appendix S1: Fig. S2).

Syndromes of germination behavior in response to after-ripening

Species were grouped into four clusters via K-means clustering analysis, and the first two principal components explained 68.8% of the variance (Fig1). These clusters represent unique patterns of dormancy change during after-ripening (Fig. 2) and germination requirements (Fig. 3) among the species. These patterns are illustrated by a representative species from each group in Figs. 2 and 3, and data for all species are shown in Appendix S1: Figs. S4, S5. Specifically, the groups are characterized by:

Cluster 1: Low $\Psi_b(50)$, low T_0, and high θ_{HT} (group averages are −1.90 MPa at 4 months after-ripening, 12°C, and 1233 MPa·°C·h, respectively). This group includes the three seed types of *Pectocarya heterocarpa* (PEHE-B, PEHE-L, PEHE-W). They are the least sensitive to low water potentials, germinate best in low temperatures, and optimal germination temperatures gradually widened during after-ripening.

Cluster 2: Moderate $\Psi_b(50)$, high T_0, and low θ_{HT} (group averages −0.81 MPa, 20°C, and 491 MPa·°C·h, respectively). This group includes *Erodium cicutarium* (ERCI), *Erodium texanum* (ERTE), *Eriophyllum lanosum* (ERLA), *Plantago patagonica* (PLPA), *Pectocarya recurvata* (PERE), *Stylocline micropoides* (STMI), and *Plantago ovata* var. *insularis* (PLIN). These species do not germinate well at lower water potentials (e.g., when Ψ < −0.8 MPa) and germinate best at warm temperatures (except for PERE). Fresh seeds germinate best at

TABLE 1. HTT parameters and model fits for seeds after-ripened in field conditions for different durations.

Species	VUOC	EUMI	DRCU	EVMU	SCBA	ERLA	PEHE-B	PEHE-L	PEHE-W	PERE	STMI	PLPA	PLIN	ERCI	ERTE
(a) 4 or 5.5-month HTT															
θ_{HT}	887	985	1,230	2,153	806	447	991	1,181	1,527	352	583	590	594	260	609
$\Psi_b(50)$	0.19	0.07	−0.40	−0.74	−0.53	−0.48	−1.18	−1.89	−2.62	−0.69	−0.90	−1.06	−1.44	−0.34	−0.79
$\sigma_{\Psi b}$	0.51	0.26	0.45	0.35	0.28	0.41	0.59	0.68	0.69	0.26	0.25	0.16	0.36	0.17	0.28
T_b	0.00	0.00	2.03	0.00	0.00	3.86	0.00	0.00	0.00	0.00	3.63	2.01	3.72	0.00	1.03
T_0	7.70	10.0	21.1	21.0	15.3	15.0	12.0	12.0	12.0	13.0	18.5	21.0	19.0	24.0	28.0
k_T	0.04	0.04	0.19	0.07	0.14	0.12	0.17	0.17	0.21	0.10	0.17	0.31	0.26	0.05	0.25
$R^2_{(sup)}$	0.88	0.95	0.90	0.90	0.93	0.93	0.89	0.95	0.89	0.94	0.92	0.87	0.86	0.95	0.87
$R^2_{(supra)}$	0.73	0.88	0.81	0.74	0.70	0.89	0.75	0.85	0.83	0.89	0.89	0.87	0.88	0.93	0.61
(b) Months (0–5.5)															
0. $\Psi_b(50)$	−†	–	–	–	–	0.01	−0.18	−0.52	−0.66	−0.08	−0.23	−0.43	−0.6	0.04	−0.54
$\sigma_{\Psi b}$	–	–	–	–	–	0.02	0.41	0.23	0.33	0.20	0.17	0.23	0.28	0.06	0.18
R^2	–	–	–	–	–	0.96	0.99	0.87	0.94	0.94	0.97	0.92	0.98	0.71	0.88
1. $\Psi_b(50)$	–	–	−0.09	−0.20	–	0.29	−0.43	−1.01	−1.44	−0.31	−0.58	−0.09	−0.47	−0.23	−0.72
$\sigma_{\Psi b}$	–	–	0.22	0.34	–	0.48	0.37	0.34	0.45	0.16	0.15	0.22	0.36	0.21	0.20
R^2	–	–	0.82	0.99	–	0.90	0.99	0.99	0.99	0.98	0.96	0.82	0.99	0.98	0.97
2. $\Psi_b(50)$	–	–	−0.1	−0.24	–	0.05	−0.48	−1.01	−1.57	−0.42	−0.68	−0.65	−0.33	−0.24	−0.67
$\sigma_{\Psi b}$	–	–	0.13	0.24	–	0.40	0.45	0.36	0.21	0.20	0.16	0.15	0.32	0.28	0.17
R^2	–	–	0.99	0.99	–	0.96	0.96	0.94	0.72	0.98	0.97	0.97	0.97	0.94	0.85
3. $_b(50)$	0.13	–	−0.63	−0.54	0.41	−0.05	−0.69	−1.14	−2.45	−0.68	−1.02	−0.98	−1.17	−0.28	−1.11
Ψ_b	0.65	–	0.33	0.27	0.60	0.61	0.38	0.54	0.69	0.30	0.38	0.17	0.48	0.28	0.37
R^2	0.92	–	0.83	0.95	0.94	0.86	0.99	0.98	0.99	0.95	0.94	0.90	0.96	0.89	0.98
4. $_b(50)$	0.12	0.05	−0.41	−0.66	−0.53	−0.45	−1.01	−1.83	−2.72	−0.71	−0.86	−0.95	−1.5	−0.32	−0.85
Ψ_b	0.48	0.35	0.3	0.27	0.22	0.37	0.43	0.70	0.75	0.25	0.22	0.09	0.42	0.20	0.33
R^2	0.96	0.95	0.92	0.96	0.98	0.89	0.98	0.97	0.99	0.98	0.97	0.90	0.94	0.95	0.96
5.5 $_b(50)$	−0.03	0.05	–	–	−0.18	–	–	–	–	–	–	–	–	–	–
Ψ_b	0.48	0.24	–	–	0.18	–	–	–	–	–	–	–	–	–	–
R^2	0.87	0.77	–	–	0.98	–	–	–	–	–	–	–	–	–	–

Notes: The 0–3 month seeds were only tested at one water potential (0 MPa). Therefore, for these months θ_{HT} and T_b were from the 4 or 5.5m HTT results (a) and kept constant while $\Psi_b(50)$ and $\sigma_{\Psi b}$ were allowed to vary until a best fit was found and the residuals between observed germination fraction and predicted germination fraction were minimized (b). Same procedure was also applied to 4–5.5 months (excluding water potential treatments other than in water) (b) for comparison with (a).

† Insufficient germination data for parameter estimation.

cool temperatures (except for ERTE, which exhibited little dormancy) and optimal germination temperatures gradually widened during after-ripening. Physical constraints to germination were removed for ERCI and ERTE by removal of the seed/fruit coats, so results represent only physiological dormancy, which was rapidly alleviated by after-ripening in these species.

Cluster 3: High $\Psi_b(50)$, high T_0, and very high θ_{HT} (group averages −0.57 MPa, 21°C, and 1,692 MPa·°C·h, respectively). This group includes *Draba cuneifolia* (DRCU) and *Evax multicaulis* (EVMU). They are sensitive to low water potentials, prefer warm temperatures, and are slow germinants because of the combination of high $\Psi_b(50)$ and θ_{HT} values. Fresh seeds are largely dormant, and both maximum germination percentages and optimal temperature range increase significantly as after-ripening progresses.

Cluster 4: Very high $\Psi_b(50)$, low T_0, and moderate θ_{HT} (group averages −0.09MPa, 11°C, and 893 MPa·°C·h, respectively). This group includes *Eucrypta micrantha* (EUMI), *Festuca octiflora* (VUOC), and *Schismus barbatus* (SCBA). Seeds are highly dormant at harvest and a majority of the seed population remained dormant after 5.5 months of after-ripening (maximum g < 50% in water). An exception is SCBA, in which the maximum g reached above 75% at 4-months field after-ripening but decreased to below 50% again at 5.5 months.

HTT parameters and germination ecology in the field

Using HTT model parameters from the field–after-ripened seeds, we estimated germination rates (GR(16)) and after-ripening rates (AR(16)) for the 16% germination percentile at 0 MPa and 10°C (Appendix S1: Fig. S3). GR(16) varied between 0.003 and 0.027 h^{-1} for 4-month–after-ripened seeds while maximum AR (16) varied between 0.003 and 0.016 h^{-1}. Across species, higher field germination fractions and earlier mean field germination dates were associated with lower θ_{HT}, higher maximum AR(16), and higher GR(16) values across months (Fig. 4; only θ_{HT} and AR(16) are shown; model parameters of the three seed types of PEHE were averaged, as field data for separate seed types were not available). Lower θ_{HT} and higher GR(16) values generally indicate more rapid germination, and higher values of maximum AR(16) suggest higher capacities for dormancy loss during after-ripening. A GR(16) smaller than 0.008 (Appendix S1: Fig. S3) indicates that less than 16% of the seed population would germinate within 5 d even with abundant moisture. Thus, germination fraction in the field for a seed population in this physiological state (e.g., VUOC, EUMI, and DRCU) is expected to be small, given that seeds are usually located near the soil surface, where water potential decreases quickly after rainfall. This is in accordance with 25-yr averages
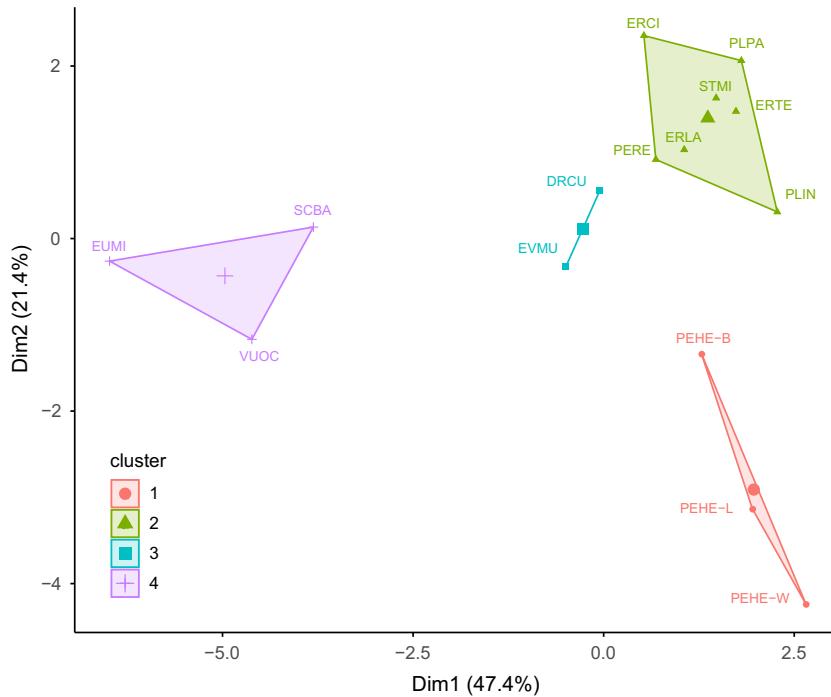
FIG. 1. K-means clustering analysis and principal component analysis results on HTT model parameters (θ_{HT}, T_b, T_0, k_T, $\Psi_b(50)$, and $\Psi_b(50)$ and $\sigma_{\Psi b}$ for seeds after-ripened from 0 to 4 months) of 15 desert annual plant species. Data are plotted according to the first two principal components that explain the majority of the variance.

of field germination fractions (0.36, 0.24, and 0.29 for VUOC, EUMI, and DRCU, respectively). In contrast, species with high GR(16) values such as ERCI and ERTE can achieve 16% of germination within 2 d and thus are likely to have high-germination fractions in the field. This also agrees well with the long-term field germination data, in which these two species exhibited the highest germination fractions (Fig. 4). We did not find significant correlations between field germination traits and $\Psi_b(50)$ values during after-ripening. However, AR (16) is indicative of changes in $\Psi_b(50)$ and $\sigma_{\Psi b}$ (Eqs. 7 and 8).

DISCUSSION

The diverse germination syndromes observed in this guild of species illustrate the multiple ways that winter annuals avoid germinating with summer monsoon rains and synchronize germination with appropriate seasonal growing conditions (Question 1). The overall good fit of HTT models to our growth chamber germination data indicates that they successfully integrate germination responses to temperature and water availability (Table 1, Appendix S1: Fig. S1; Question 2). Furthermore, the significant correlations of long-term field germination observations with HTT parameters (Fig. 4) suggests that they are effective descriptors of germination physiologies for mechanistically characterizing the contribution of germination to population dynamics (Question 3).

Hydrothermal time constants (θ_{HT}), maximum after-ripening rates (AR), and germination rates (GR) from field–after-ripened seeds were significantly correlated with long-term field measurements of germination success (field germination fractions and germination dates). The germination niches simulated from hydrothermal parameters match well to the field-observed germination niches of several species (e.g., EVMU, PERE, PLIN) in the same system (Kimball et al. 2010).

In a few species, some of the germination responses at lower water potentials deviated noticeably from the fitted curves. This may be due to increased sensitivity to T at lower Ψ, or to the presence of subpopulations with different distributions of base water potentials (e.g., PEHE-L at −0.4 MPa, 18–20°C in Appendix S1: Fig. S1-I). In addition, we assumed the base temperature threshold values remained constant during after-ripening, which may not always be the case, as shifts in temperature sensitivity also constitute a seed dormancy mechanism (Batlla and Benech-Arnold 2015). Nonetheless, for this guild of desert annuals, water is the main limiting resource and temporal variation in rainfall is much greater and more unpredictable than that of temperature. Thus, shifting of $\Psi_b(50)$ to lower values likely constitutes the most significant physiological response accounting for loss of primary dormancy. However, despite negative shifts in $\Psi_b(50)$ during after-ripening when imbibed at lower temperatures, the cool-germinating species (e.g., PEHE and PERE) were still unable to
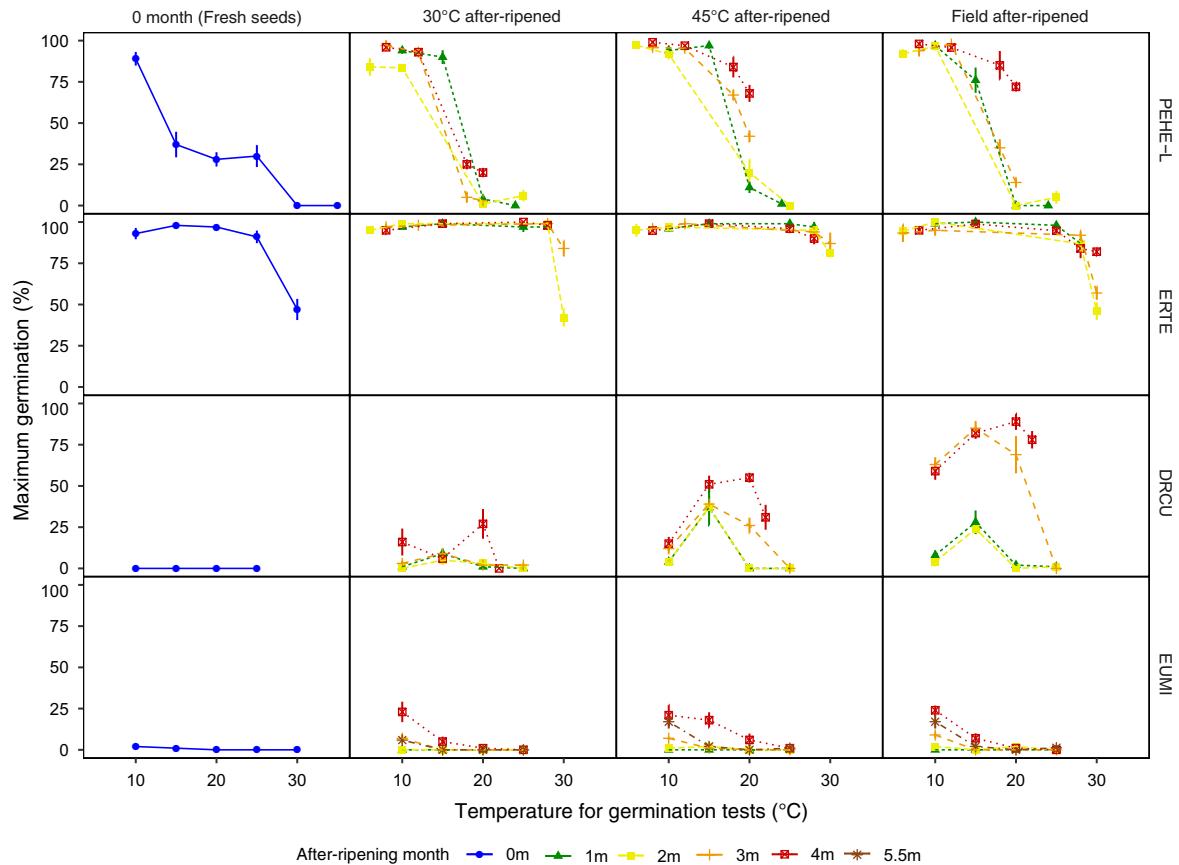
FIG. 2. Maximum germination percentages for four desert annual species (illustrative of the four syndromes identified by clustering analysis) across a range of incubation temperatures and after-ripening durations. Seeds were after-ripened at three conditions (30°C, 45°C or in the field) for 0 (fresh seeds), 1, 2, 3, and 4 months (and for an additional 1.5 months for EUMI). Error bars indicate ± SE.

germinate well at warmer temperatures (i.e., exhibited "thermoinhibition"). Even as these seeds became increasingly capable of rapid germination at cool temperatures, they retained the fail-safe of germination inhibition at warm temperatures, preventing premature germination during the monsoon season.

After-ripening did not always have consistent, incremental effects in all species, as illustrated by changes in germination rate (GR) and quantified as after-ripening rate (AR; i.e., change in slopes of GR between months; Appendix S1: Fig. S3). Interestingly, for field–after-ripened seeds, nine of the species (including winged seed of PEHE but not the two other seed types) had maximum AR between the 2nd and 3rd (3rd and 4th in EUMI and SCBA) months, and eight species had a very small or negative AR between the 3rd and 4th (4th and 5.5th in EUMI and SCBA) months, indicating that dormancy remained constant or the seed population became more dormant than the previous month. Storage periods between the second and third months (mid-July to mid-August) would coincide with the summer monsoon season. Variation in both temperature and relative

humidity is greater during the monsoon season, which may affect the seasonal changes of AR. In addition, as noted above, thermoinhibition at warm temperatures can be retained even when dormancy at lower temperatures is alleviated (Huo and Bradford 2015). Thus, primary dormancy that prevents premature germination following seed shedding at cooler temperatures is alleviated by after-ripening, but thermoinhibition can be retained to block germination when water is adequate but temporary, as during the summer monsoon.

Within-group variation in germination syndromes may also indicate differences in adaptive strategies, such as the three seed types of PEHE, which were grouped in the same cluster. Seed heteromorphism was proposed to confer a selective advantage to plants that grow in extreme and variable environments, such as via providing more seedling cohorts to spread the risks of survival (Venable 1985, Yang et al. 2017). For example, the winged seed (PEHE-W) had the lowest $\Psi_b(50)$ among the three seed types across months, which suggests that they may function as the "explorer" propagules to adapt to longer dispersal distances and more stressful
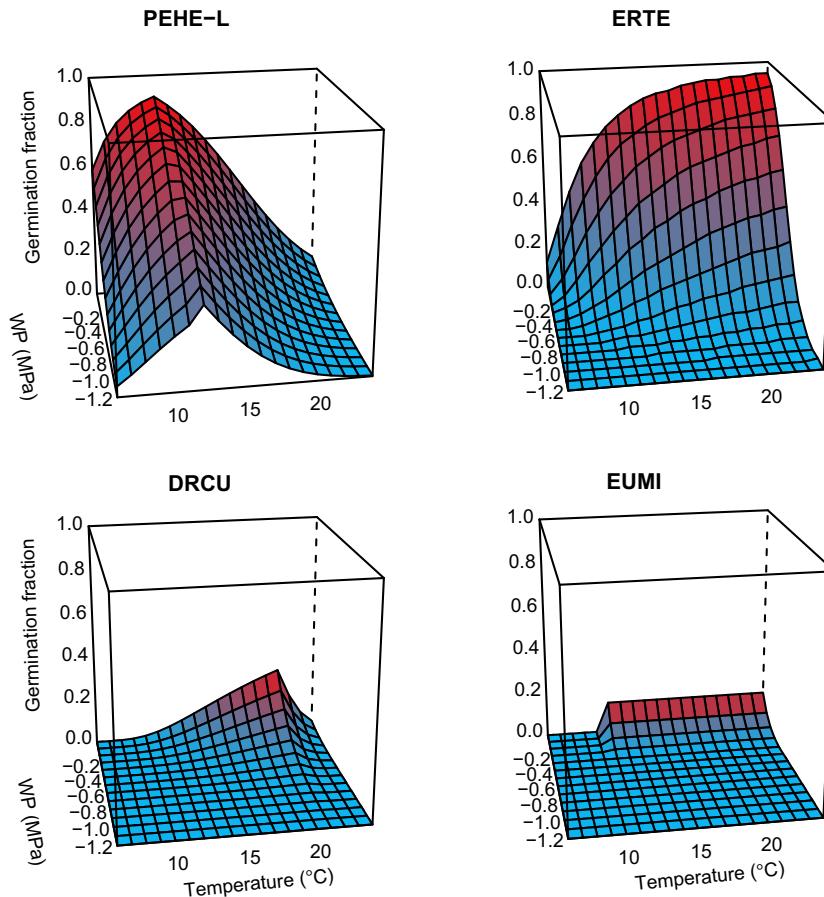
FIG. 3. Simulated germination fractions within 5 d of incubation for four desert annual species (illustrative of the four syndromes identified by clustering analysis) in a matrix of water potentials and temperatures. Simulations were generated by the HTT model after 4 or 5.5 months (for EUMI) of field after-ripening.

conditions. In contrast, the more positive $\Psi_b(50)$ in basal seeds may suggest a more conservative germination strategy (i.e., germinable only at higher environmental water potentials), as these seeds usually stay underground near the maternal plant and face intense between- and within-species competition from the seed bank (Appendix S1: Fig. S2; cf. predictions of dormancy-dispersal correlations in Venable and Brown 1988).

The fluctuations of AR may continue over years as seeds reside in the soil seed bank (commonly viewed as secondary dormancy or dormancy cycling after the first year), and result in unique species-time dynamics of dormancy states in response to seasonal climate variation (Footitt et al. 2014, 2015). The dynamic after-ripening patterns among species within a community may add an additional layer of variation in germination timing, which could further diversify germination niches within and among species, and both within and across seasons (Donohue et al. 2010).

Using adaptive dynamic models for species of the same community, Gremer et al. (2016) showed that

spreading germination within and among years is generally beneficial, and that these species may adopt integrative strategies combining predictive plasticity in germination fractions or timing with bet hedging. Early vs. late germination fractions in the field as well as overall germination fractions vary from year to year in an adaptive way. During years when more seeds tended to germinate early in the season, early germinants tended to have higher lifetime fitness, suggesting predictive plasticity in germination timing in addition to bet hedging. Seeds also tended to germinate to higher fractions in years with good survival and fecundity (Gremer et al. 2016). HTT parameters are likely good descriptors for such strategies. For example, higher germination plasticity (i.e., broader germination niches) may be achieved when $\Psi_b(g)$ has a lower median value ($\Psi_b(50)$) and a larger standard deviation ($\sigma_{\Psi b}$; e.g., compare germination of PEHE-L and ERTE across a gradient of water potentials; Table 1, Fig. 3). This could result in large differences in germination fractions in different years or spreading germination across multiple rain events in a given year, leading to predictive (plastic) germination
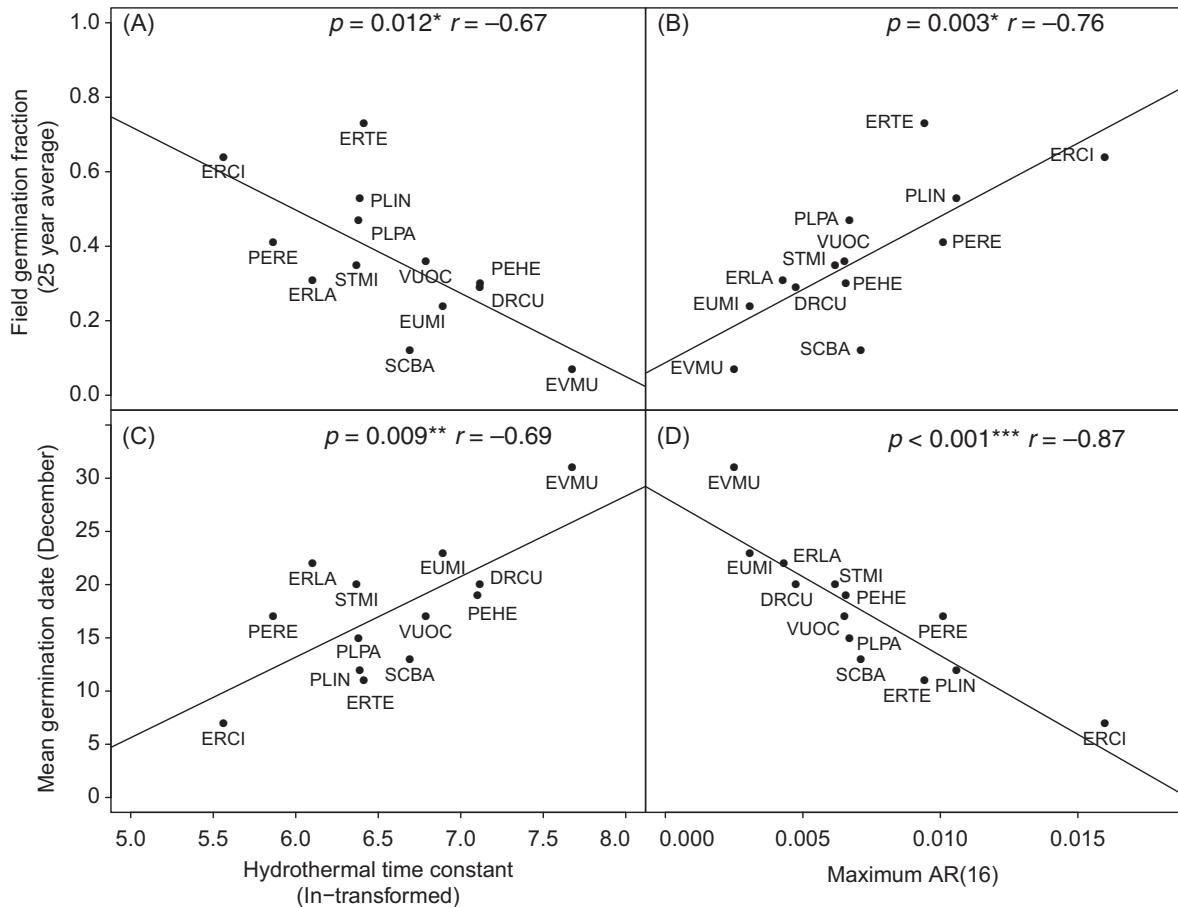
FIG. 4. Relationships between field germination patterns (25-yr averages for mean germination date and germination fraction) and HTT model-derived parameters (hydrothermal time constant, panels A, B; and maximum after-ripening rate, panels C, D) for seeds after-ripened for 4 months in the field. Correlation equations are (A) $y = 1.84 - 0.22x$; (B) $y = -32.24 + 7.57x$; (C) $y = 0.087 + 39.28x$; (D) $y = 28.15 - 1{,}481.98x$. Significance codes: $*P < 0.05$, $**P < 0.01$, $***P < 0.001$.

and/or within-year bet hedging. Meanwhile, combinations of HTT parameters that lead to more consistent (small fluctuations) and lower GR across after-ripening time (within or among years) may cause more evenly distributed germination across years, indicating a stronger component for between-year bet hedging or less plasticity for germination fraction (e.g., EUMI; Table 1, Fig. 2, Fig. 4B, Appendix S1: Fig. S3). Thus, a species' germination strategy may be represented by its after-ripening pattern, which is essentially the coordination between the combinations of HTT parameters (in particular θ_{HT}, T_b, $\Psi_b(50)$ and $\sigma_{\Psi b}$) at a certain dormancy state and the changes in these parameters in response to after-ripening time and conditions. The physiological sensitivity to environmental conditions, evolutionarily integrated through the HTT mechanism, allows germination timing to vary within and between years in an adaptive way.

A consistent after-ripening pattern (shown as the changes of GR over time, Appendix S1: Fig. S3) is generally observed for each species, despite some variation across the three after-ripening conditions. This suggests

that after-ripening pattern is a species-specific trait that correlates germination timing with other species-specific life history traits. Functional correlations and trade-offs are important in this desert annual community and contribute to the species-by-year interaction underpinning species coexistence via a storage effect (Angert et al. 2009) and to climate-driven shifts in community composition (Kimball et al. 2010, 2011). Angert et al. (2009) demonstrated coexistence via the storage effect, half of which was promoted by species differences in germination response to temporal environmental variation. The species-specific after-ripening and germination traits documented here provide the functional basis of such germination decoupling between species. Huang et al. (2016) further demonstrated that low-germination fraction species (e.g., DRCU and EVMU, Fig. 4), are associated with low integrated water-use efficiency, high growth rate, and smaller seeds. These species exhibited slow-germinating traits such as large hydrothermal time constants, low field-germination fraction, and late germination date, and are also characterized by more

constant after-ripening patterns because of lower GR and maximum AR (Fig. 4, Appendix S1: Fig. S3). In the field, species with this syndrome tend to have high fitness variation from year to year, which is buffered by bet-hedging in the form of their low germination fractions. In contrast, high-germination fraction species, such as PERE and PLIN, are associated with high integrated water-use efficiency, slow growth rate, and larger seeds. Such species have higher GR in fresh seeds and a more significant increase in GR during after-ripening. They tend to have lower fitness variation from year to year, and hence require less bet hedging in the form of delayed fractional germination.

Some intriguing questions remain unanswered. For instance, it is not clear how the HTT sensitivity distributions and kinetics of germination allow species to vary within- and between-year timing of germination in an adaptive way, synchronizing germination with fitness opportunities (Gremer et al. 2016). Similarly, it is also unknown how these fitness consequences of dormancy relate to maternal environmental effects on dormancy expression (Donohue 2009, Chen et al. 2014, Piskurewicz et al. 2016, Auge et al. 2017). How has selection on dormancy cycling contributed to niche differentiation and diversity maintenance of coexisting species (Chesson et al. 2004, Angert et al. 2009)? With HTT modeling, after-ripening patterns can be quantitatively integrated into the "functional trait-population dynamic-community dynamic" framework (Huxman et al. 2013, Huang et al. 2016), thus offering novel information to address these issues. The advances reported here relating HTT controls on germination with ecological patterns of germination observed in the field should improve our ability to predict vegetation responses to environmental change and enable more mechanistic ecological modeling of plant populations and communities.

LITERATURE CITED

Adondakis, S., and D. L. Venable. 2004. Dormancy and germination in a guild of Sonoran Desert annuals. Ecology 85:2582–2590.

Allen, P. S., and S. E. Meyer. 2002. Ecology and ecological genetics of seed dormancy in downy brome. Weed Science 50:241–247.

Allen, P. S., S. E. Meyer, and M. A. Khan. 2000. Hydrothermal time as a tool in comparative germination studies. Pages 401–410 in M. Black, K. J. Bradford, and J. Vazquez-Ramos, editors. Seed biology: advances and applications. CABI, Wallingford, UK.

Allen, P., L. Benech-Arnold, D. Batlla, and K. Bradford. 2007. Modeling seed dormancy. Pages 72–112 in K. J. Bradford and H. Nonogaki, editors. Seed development, dormancy and germination. Blackwell Publishing Ltd, Oxford, UK.

Alvarado, V., and K. J. Bradford. 2002. A hydrothermal time model explains the cardinal temperatures for seed germination. Plant, Cell and Environment 25:1061–1069.

Alvarado, V., and K. J. Bradford. 2005. Hydrothermal time analysis of seed dormancy in true (botanical) potato seeds. Seed Science Research 15:77–88.

Angert, A. L., T. E. Huxman, P. Chesson, and D. L. Venable. 2009. Functional tradeoffs determine species coexistence via the storage effect. Proceedings of the National Academy of Sciences of the United States of America 106:11641–11645.

Auge, G. A., L. D. Leverett, B. R. Edwards, and K. Donohue. 2017. Adjusting phenotypes via within- and across-generational plasticity. New Phytologist 216:343–349.

Baskin, J., and C. Baskin. 1985. The annual dormancy cycle in buried weed seeds: a continuum. BioScience 35:492–498.

Baskin, C., and J. Baskin. 2014. Seeds: ecology, biogeography, and evolution of dormancy and germination. Second edition. Academic Press, San Diego, California, USA.

Baskin, C., J. Chesson, and J. Baskin. 1993. Annual seed dormancy cycles in two desert winter annuals. Journal of Ecology 81:551–556.

Batlla, D., and A. M. Agostinelli. 2017. Thermal regulation of secondary dormancy induction in *Polygonum aviculare* seeds: a quantitative analysis using the hydrotime model. Seed Science Research 27:231–242.

Batlla, D., and R. L. Benech-Arnold. 2015. A framework for the interpretation of temperature effects on dormancy and germination in seed populations showing dormancy. Seed Science Research 25:147–158.

Bauer, M. C., S. E. Meyer, and P. S. Allen. 1998. A simulation model to predict seed dormancy loss in the field for *Bromus tectorum* L. Journal of Experimental Botany 49:1235–1244.

Bazin, J., N. Langlade, P. Vincourt, S. Arribat, S. Balzergue, H. El-Maarouf-Bouteau, and C. Bailly. 2011. Targeted mRNA oxidation regulates sunflower seed dormancy alleviation during dry after-ripening. The Plant Cell 23:2196–2208.

Bello, P., and K. J. Bradford. 2016. Single-seed oxygen consumption measurements and population-based threshold models link respiration and germination rates under diverse conditions. Seed Science Research 26:199–221.

Bewley, J., K. Bradford, H. Hilhorst, and H. Nonogaki. 2013. Seeds: physiology of development, germination and dormancy. Third edition. Springer, New York, New York, USA.

Bliss, C. I. 1934. The method of probits. Science 79:38–39.

Bloomberg, M., J. R. R. Sedcole, E. G. G. Mason, and G. Buchan. 2009. Hydrothermal time germination models for radiata pine (*Pinus radiata* D. Don). Seed Science Research 19:171–182.

Bradford, K. J. 1990. A water relations analysis of seed germination rates. Plant Physiology 94:840–849.

Bradford, K. J. 1995. Water relations in seed germination. Pages 351–396 in J. Kigel and G. Galili, editors. Seed development and germination. Marcel Dekker, New York, New York, USA.

Bradford, K. J. 2002. Applications of hydrothermal time to quantifying and modeling seed germination and dormancy. Weed Science 50:248–260.

Bradford, K. J. 2018. Interpreting biological variation: seeds, populations and sensitivity thresholds. Seed Science Research 28:158–167.

Cao, D., C. C. Baskin, J. M. Baskin, F. Yang, and Z. Huang. 2014. Dormancy cycling and persistence of seeds in soil of a cold desert halophyte shrub. Annals of Botany 113:171–179.

de Casas, R. R., K. Kovach, E. Dittmar, D. Barua, B. Barco, and K. Donohue. 2012. Seed after-ripening and dormancy determine adult life history independently of germination timing. New Phytologist 194:868–879.

Chen, M., D. R. MacGregor, A. Dave, H. Florance, K. Moore, K. Paszkiewicz, N. Smirnoff, I. A. Graham, and S. Penfield. 2014. Maternal temperature history activates Flowering Locus T in fruits to control progeny dormancy according to time of year. Proceedings of the National Academy of Sciences of the United States of America 111:18787–18792.

Chesson, P., R. L. E. Gebauer, S. Schwinning, N. Huntly, K. Wiegand, M. S. K. Ernest, A. Sher, A. Novoplansky, and J. F. Weltzin. 2004. Resource pulses, species interactions, and diversity maintenance in arid and semi-arid environments. Oecologia 141:236–253.

Christensen, M., S. E. Meyer, and P. S. Allen. 1996. A hydrothermal time model of seed after-ripening in Bromus tectorum L. Seed Science Research 6:155–164.

Clauss, M. J., and D. L. Venable. 2000. Seed germination in desert annuals: an empirical test of adaptive bet hedging. American Naturalist 155:168–186.

Cohen, D. 1966. Optimizing reproduction in a randomly varying environment. Journal of Theoretical Biology 12:119–129.

Copete, M. A., J. M. Herranz, P. Ferrandis, and E. Copete. 2015. Annual dormancy cycles in buried seeds of shrub species: Germination ecology of Sideritis serrata (Labiatae). Plant Biology 17:798–807.

Dahal, P., and K. J. Bradford. 1994. Hydrothermal time analysis of tomato seed germination at suboptimal temperature and reduced water potential. Seed Science Research 4:71–80.

Donohue, K. 2002. Germination timing influences natural selection on life-history characters in Arabidopsis thaliana. Ecology 83:1006–1016.

Donohue, K. 2009. Completing the cycle: maternal effects as the missing link in plant life histories. Philosophical Transactions of the Royal Society B 364:1059–1074.

Donohue, K., L. Dorn, C. Griffith, E. Kim, A. Aguilera, C. R. Polisetty, and J. Schmitt. 2005. Niche construction through germination cueing: life-history responses to timing of germination in Arabidopsis thaliana. Evolution 59:771–785.

Donohue, K., R. Rubio de Casas, L. Burghardt, K. Kovach, and C. G. Willis. 2010. Germination, postgermination adaptation, and species ecological ranges. Annual Review of Ecology, Evolution, and Systematics 41:293–319.

Donohue, K., L. T. Burghardt, D. Runcie, K. J. Bradford, and J. Schmitt. 2015. Applying developmental threshold models to evolutionary ecology. Trends in Ecology and Evolution 30:66–77.

Dürr, C., J. B. Dickie, X. Y. Yang, and H. W. Pritchard. 2015. Ranges of critical temperature and water potential values for the germination of species worldwide: Contribution to a seed trait database. Agricultural and Forest Meteorology 200:222–232.

Finch-Savage, W. E., and S. Footitt. 2017. Seed dormancy cycling and the regulation of dormancy mechanisms to time germination in variable field environments. Journal of Experimental Botany 68:843–856.

Finch-Savage, W. E., and G. Leubner-Metzger. 2006. Seed dormancy and the control of germination. New Phytologist 171:501–523.

Finch-Savage, W. E., H. R. Rowse, and K. C. Dent. 2005. Development of combined imbibition and hydrothermal threshold models to simulate maize (Zea mays) and chickpea (Cicer arietinum) seed germination in variable environments. New Phytologist 165:825–838.

Footitt, S., Clay, H. A., K. Dent, and W. E. Finch-Savage 2014. Environment sensing in spring-dispersed seeds of a winter annual Arabidopsis influences the regulation of dormancy to align germination potential with seasonal changes. New Phytologist 202:929–939.

Footitt, S., K. Müller, A. R. Kermode, and W. E. Finch-Savage. 2015. Seed dormancy cycling in Arabidopsis: Chromatin remodelling and regulation of DOG1 in response to seasonal environmental signals. Plant Journal 81:413–425.

Galloway, L. F. 2001. Parental environmental effects on life-history in the herbaceous plant Campanula americana. Ecology 82:2781–2789.

Galloway, L. F. 2002. The effect of maternal phenology on offspring characters in the herbaceous plant Campanula americana. Journal of Ecology 90:851–858.

Garcia-Huidobro, J., J. L. Monteith, and R. Squire. 1982. Time, temperature and germination of pearl millet (Pennisetum typhoides S and H.). I. Constant temperature. Journal of Experimental Botany 33:297–300.

Gremer, J. R., and D. L. Venable. 2014. Bet hedging in desert winter annual plants: optimal germination strategies in a variable environment. Ecology Letters 17:380–387.

Gremer, J. R., S. Kimball, and D. L. Venable. 2016. Within- and among-year germination in Sonoran Desert winter annuals: bet hedging and predictive germination in a variable environment. Ecology Letters 19:1209–1218.

Grundy, A. C., K. Phelps, R. J. Reader, and S. Burston. 2000. Modelling the germination of Stellaria media using the concept of hydrothermal time. New Phytologist 148:433–444.

Gummerson, R. J. 1986. The effect of constant temperatures and osmotic potentials on the germination of sugar beet. Journal of Experimental Botany 37:729–741.

Holdsworth, M. J., L. Bentsink, and W. J. J. Soppe. 2008. Molecular networks regulating Arabidopsis seed maturation, after-ripening, dormancy and germination. New Phytologist 179:33–54.

Huang, Z., S. Liu, K. J. Bradford, T. E. Huxman, and D. L. Venable. 2016. The contribution of germination functional traits to population dynamics of a desert plant community. Ecology 97:250–261.

Huo, H., and K. J. Bradford. 2015. Molecular and hormonal regulation of thermoinhibition of seed germination. Pages 3–33 in J. V. Anderson, editor. Advances in plant dormancy. Springer, New York, New York, USA.

Huo, H., S. Wei, and K. J. Bradford. 2016. DELAY OF GERMINATION1 (DOG1) regulates both seed dormancy and flowering time through microRNA pathways. Proceedings of the National Academy of Sciences of the United States of America 115:E2199–E2206.

Huxman, T. E., Kimball, S., Angert, A. L., Gremer, J. R., Barron-Gafford, G. A. and Venable, D. L. 2013. Understanding past, contemporary, and future dynamics of plants,

populations, and communities using Sonoran Desert winter annuals. American Journal of Botany 100:1369–1380.

Kebreab, E., and A. J. Murdoch. 1999. Modelling the effects of water stress and temperature on germination rate of *Orobanche aegyptiaca* seeds. Journal of Experimental Botany 50:655–664.

Kimball, S., A. L. Angert, T. E. Huxman, and D. L. Venable. 2010. Contemporary climate change in the Sonoran Desert favors cold-adapted species. Global Change Biology 16:1555–1565.

Kimball, S., A. L. Angert, T. E. Huxman, and D. L. Venable. 2011. Differences in the timing of germination and reproduction relate to growth physiology and population dynamics of Sonoran Desert winter annuals. American Journal of Botany 98:1773–1781.

Köchy, M., and K. Tielbörger. 2007. Hydrothermal time model of germination: parameters for 36 Mediterranean annual species based on a simplified approach. Basic and Applied Ecology 8:171–182.

Lasdon, L. S., A. D. Waren, A. Jain, and M. Ratner. 1978. Design and testing of a generalized reduced gradient code for nonlinear programming. ACM Transactions on Mathematical Software 4:34–50.

Long, R. L., M. J. Gorecki, M. Renton, J. K. Scott, L. Colville, D. E. Goggin, L. E. Commander, D. A. Westcott, H. Cherry, and W. E. Finch-Savage. 2015. The ecophysiology of seed persistence: a mechanistic view of the journey to germination or demise. Biological Reviews 90:31–59.

Mesgaran, M. B., A. Onofri, H. R. Mashhadi, and R. D. Cousens. 2017. Water availability shifts the optimal temperatures for seed germination: a modelling approach. Ecological Modelling 351:87–95.

Meyer, S. E., and P. S. Allen. 2009. Predicting seed dormancy loss and germination timing for *Bromus tectorum* in a semi-arid environment using hydrothermal time models. Seed Science Research 19:225.

Michel, B. E. 1983. Evaluation of the water potentials of polyethylene glycol 8000 both in the presence and absence of other solutes. Plant Physiology 72:66–70.

Onofri, A., P. Benincasa, M. B. Mesgaran, and C. Ritz. 2018. Hydrothermal-time-to-event models for seed germination. European Journal of Agronomy 101:129–139.

Piskurewicz, U., M. Iwasaki, D. Susaki, C. Megies, T. Kinoshita, and L. Lopez-Molina. 2016. Dormancy-specific imprinting underlies maternal inheritance of seed dormancy in *Arabidopsis thaliana*. eLife 5:1–23.

Roberts, E. H. 1973. Predicting the storage life of seeds. Seed Science & Technology 1:499–514.

Rowse, H., and W. Finch-Savage. 2003. Hydrothermal threshold models can describe the germination response of carrot (*Daucus carota*) and onion (*Allium cepa*) seed populations across both sub- and supra-optimal temperatures. New Phytologist 158:101–108.

Simons, A. M. 2011. Modes of response to environmental change and the elusive empirical evidence for bet hedging. Proceedings of the Royal Society B 278:1601–1609.

Venable, D. L. 1985. The evolutionary ecology of seed heteromorphism. American Naturalist 126:577–595.

Venable, D. L. 1999. Population ecology of Sonoran Desert annual plants. Pages 115–142 *in* R. Robichaux, editor. Ecology of Sonoran Desert plants and plant communities. The University of Arizona Press, Tucson, Arizona, USA.

Venable, D. L. 2007. Bet hedging in a guild of desert annuals. Ecology 88:1086–1090.

Venable, D. L., and J. S. Brown. 1988. The selective interactions of dispersal, dormancy, and seed size as adaptations for reducing risk in variable environments. American Naturalist 131:360–384.

Venable, D. L., and C. E. Pake.1999. Population ecology of Sonoran Desert annual plants. Pages 115–142 in R. Robichaux, editor. Ecology of sonoran desert plants and plant communities. The University of Arizona Press, Tucson, Arizona, USA.

Watt, M. S., and M. Bloomberg. 2012. Key features of the seed germination response to high temperatures. New Phytologist 196:332–336.

Watt, M. S., M. Bloomberg, and W. E. Finch-Savage. 2011. Development of a hydrothermal time model that accurately characterises how thermoinhibition regulates seed germination. Plant, Cell and Environment 34:870–876.

Yang, F., J. M. Baskin, C. C. Baskin, X. J. Yang, D. C. Cao, and Z. Huang. 2017. Divergence in life history traits between two populations of a seed-dimorphic halophyte in response to soil salinity. Frontiers in Plant Science 8:1–11.

SUPPORTING INFORMATION

Additional supporting information may be found in the online version of this article at http://onlinelibrary.wiley.com/doi/10.1002/ecy.2958/suppinfo